C.P. No. 774

C.P. No. 774

MINISTRY OF AVIATION

AERONAUTICAL RESEARCH COUNCIL

CURRENT PAPERS

The Pressure Distribution at Zero-Lift on Some Slender Delta Wings at Supersonic Speeds

by

M. C. P. Firmin

LONDON: HER MAJESTY'S STATIONERY OFFICE

1964

SEVEN SHILLINGS NET

U.D.C. No. 533.6.048.2 : 533.6.013.13 : 533.693.3 : 533.6.011.5

C.P. No.774

November 1963

THE PRESSURE DISTRIBUTION AT ZERO-LIFT ON SOME SLENDER DELTA WINGS AT SUPERSONIC SPEEDS

by

M. C. P. Firmin

SUMMARY

The pressure distribution has been measured on the rear of a slender delta wing with rhombic cross-sections as part of a programme to investigate the influence on the wave drag of thickness distributions that give rise to a marked adverse pressure gradient and a relatively large suction near the trailing edge.

Even for such 'non-smooth' thickness distributions, thin-wing theory gives fair results. It has, however, been found that a form of second-order inviscid perturbation theory (not-so-thin wing theory) gives much more reliable results. Slender-wing theories, on the other hand, can be most misleading for such thickness distributions.

The second-order theory has also been applied to other thickness distributions and has been found to give more reliable results than thin-wing theory except near the wing leading edges where both methods fail.

Replaces R.A.E. Tech Note No. Aero 2926 - A.R.C. 25 708.

CONTENTS

		Page
1	INTRODUCTION	3
2	DESCRIPTION OF THE MODEL	3
3	EXPERIMENTAL DETAILS	4
	3.1 Wind tunnel	4
	3.2 Accuracy	4
	3.2.1 Flow	4
	3.2.2 Measurements	4
4	EXPERIMENTAL RESULTS	5
5	ESTIMATION OF PRESSURE COEFFICIENTS	5
	5.1 Thin wing theory	5
	5.2 A 'not-so-thin' wing theory	5
6	DISCUSSION	9
7	CONCLUSIONS	12
SYMBOLS		13
REFERENCES		14
APPENDICES 1 AND 2		17-22
ILLUSTRATIONS - Figs.1-8		-
DETACHABLE ABSTRACT CARDS		-

APPENDICES

Appendix

1 - Determination of the second order solution to the potential equation for two dimensional flow 17

2 - Determination of $\left(\frac{\partial \phi_{2b}}{\partial x}\right)_{z=z_B}$ from slender theory in terms of the difference in potential between not-so-thin-wing theory and thin wing 21

ILLUSTRATIONS

	Fig.
Model details (wing 3)	1
Non-dimensional centre line thickness distributions	2
Non-dimensional cross sectional area distributions	3
Pressure distributions - wing 3	4
Schlieren photographs - wing 3	5
Pressure distributions - 'Newby' wing	6
Pressure distributions 'Lord V' wing	7
Pressure distributions over a conical body with rhombic cross-sections ($s/c_o = 0{\cdot}25$, $\tau = 0{\cdot}385$)	8

1 INTRODUCTION

In the search for slender wings with low drag some of the original investigations were made on simple shapes such as delta wings with diamond cross-sections for which theoretical calculation and model manufacture can be more easily accomplished. The work described in this Note, which forms part of a general research programme to find wings with low volume-dependent wave drag, deals with the pressure distribution on the rear of such a wing with a larger adverse pressure gradient than on wings tested up to now, together with a large suction near the trailing edge.

The object of this test was to see whether inviscid, small-perturbation, theory can be relied upon to estimate the pressure distribution even when the pressure gradients are changing fairly rapidly along the chord.

In the series of models used for drag measurements, the results for which are published in Ref.1, the model tested here corresponds to wing 3.

2 DESCRIPTION OF THE MODEL

The details of the wing, which has a unit aspect ratio, a volume parameter (τ) of 0·05 and a centre line thickness distribution given by

$$\frac{z(\xi,0)}{c_o} = \frac{v/c_o^3}{2\ s/c_o}\,\xi(1-\xi)\,\{14{\cdot}0 + 52{\cdot}67\,\xi - 167{\cdot}33\,\xi^2 + 116{\cdot}67\,\xi^3\} \qquad (1)$$

are given in Fig.1. $\xi(\equiv x/c_o)$ is the chordwise station normalised with reference to the centre-line chord and is measured from the apex.

The model was supported from the undersurface so that at the Mach numbers at which tests were made the support should not have influenced the measurements which were made on the upper surface. The centre-line chord (c_o) was 12·00 inches and all the planform edges had a nominal 0·002 inch radius. The thickness distribution was modified slightly to include the extra thickness due to the radiused planform edges.

The centre line thickness and cross sectional area distributions are given in Figs.2 and 3 where they are compared with distributions for the now well known 'Lord V' and 'Newby' wings. Wing 3 is similar in many respects to a 'Lord V' wing but is not as smooth geometrically, and has a much larger slope near the trailing edge, which is comparable with the 'Newby' wing. The centre line thickness distribution for the 'Newby' and 'Lord V' wings are given by the following equations:-

$$\frac{z(\xi,0)}{c_o} = \frac{v/c_o^3}{2\ s/c_o}\,\xi(1-\xi)\,\{12\} \qquad \text{(Newby)} \qquad (2)$$

$$\frac{z(\xi,0)}{c_o} = \frac{v/c_o^3}{2\ s/c_o}\,\xi(1-\xi)\,\{28 - 42\,\xi + 28\,\xi^2 - 7\,\xi^3\} \qquad \text{(Lord V).} \qquad (3)$$

3 EXPERIMENTAL DETAILS

3.1 Wind tunnel

The model was mounted in the R.A.E. No.19 (18" x 18") supersonic wind tunnel which is a continuous return flow closed circuit tunnel with a nominal Mach number range of 1·4 to 2·2 with a square working section of 18 inch side at all Mach numbers. In the present tests the stagnation pressure was varied up to a maximum of 75 inches of Hg corresponding to a maximum Reynolds number of $11·3 \times 10^6$ based on the wing root chord. The stagnation temperature was kept constant for all tests at a particular Mach number such that the model remained close to normal temperature (15°C). The tunnel air was kept dry during these tests using a dry-air interchange system. The tunnel humidity was measured during the tests and no results were recorded until the humidity was less than 0·0002 lb of water per lb of dry air.

The model was mounted on a quadrant type incidence gear and a check was made during the running to see that the model remained at zero incidence for all stagnation pressures.

3.2 Accuracy

3.2.1 Flow

The supersonic nozzles used for these tests are all double sided and the Mach number distribution has been obtained but not the flow inclination. The changes of the Mach number in the empty tunnel are reasonably gradual over the region occupied by the model and are within the following limits in the region of model pressure points.

M	= 1·40	±0·005
M	= 1·58	±0·007
M	= 2·02	±0·010
M	= 2·19	±0·007

Although the flow inclinations in the tunnel have not been measured previous tests all indicate that any flow inclinations that do exist are negligible.

3.2.2 Measurements

All the pressures have been measured using capsule type manometers[2] with a nominal accuracy of ±0·015 inches of Mercury. There were, however, faults in these instruments which reduced their accuracy. A datum pressure was measured using the instruments before and after each run and if a change in instrument zero of more than 0·04 inches of Mercury occurred then the results obtained with that instrument were discarded. The remaining instruments should then have an accuracy of better than ±0·03 inches of Mercury which corresponds to a change in pressure coefficient of about ±0·001 at a Reynolds number of 10^7 for all the test Mach numbers. To obtain

a corresponding figure for a lower Reynolds number this value should be increased by the inverse ratio of the Reynolds numbers.

4 EXPERIMENTAL RESULTS

The pressures measured during these tests are given in Figs.4(a)-(d) and are presented as pressure coefficients based on the mean flow in the region of the model pressure points. All the results obtained at the highest Reynolds number for each Mach number are presented, but other results are given only if they are measurably different from those at the highest Reynolds number. All the measurements presented were obtained with free transition but a check, at $M = 2{\cdot}02$, made with transition bands of the distributed roughness type described in Ref.1 showed no measurable influence of the transition bands at the highest Reynolds number.

5 ESTIMATION OF PRESSURE COEFFICIENTS

5.1 Thin-wing theory

Thin-wing theory is the term generally accepted for the theory of inviscid irrotational flow based on the first-order linearized potential equation, in which the boundary conditions to be satisfied on the wing surface are applied in the chordal plane of the wing and the flow variables required on the wing surface are evaluated again in the chordal plane of the wing. The pressure is obtained from the first-order linearized Bernoulli equation. If, in addition, the slender approximation ($|\beta^2 \phi_{xx}| << |\phi_{yy}| + |\phi_{zz}|$) is made, then the theory is termed slender thin-wing theory.

The pressure distribution at zero lift for delta wings with rhombic cross-sections has been obtained from thin-wing theory by a numerical method by Eminton[3] using the D.E.U.C.E. digital computer, but the machine time involved was large (order of minutes per station)* so it was decided to obtain an analytical solution. This is possible if the centre line thickness distribution is restricted to polynomial form. A Mercury autocode programme has been written which obtains the first-order velocity perturbations for such wings[5]; it takes about 1 second per station.

Corresponding results for slender thin-wing theory may be obtained from the results given by Weber[6].

5.2 A not-so-thin wing theory

For 'wing like' shapes such that the local thickness is very much smaller than the local span the velocity potential Φ for irrotational, homentropic flow may be written as $\Phi = U(x + \phi_1 + \phi_2 + O(t^3))$, where ϕ_1, ϕ_2 etc. are proportional to the wing thickness, square of the wing thickness etc. Equating terms of the same order in thickness the differential equations satisfied by the velocity perturbations are

---

*A Mercury autocode programme[4] for the thin-wing theory pressure distribution on wings of more complex cross sections and planform using numerical methods now exists and takes about 1 minute per station.

$$\nabla^2 \phi_1 - M^2 \frac{\partial^2 \phi_1}{\partial x^2} = 0 \qquad (4)$$

$$\nabla^2 \phi_2 - M^2 \frac{\partial^2 \phi_2}{\partial x^2} = M^2 \frac{\partial}{\partial x} (\nabla \phi_1)^2 + (\gamma - 1) M^2 \frac{\partial \phi_1}{\partial x} \nabla^2 \phi_1 \qquad (5)$$

where ϕ_1 is the first-order perturbation velocity potential and ϕ_2 is a second-order correction to it (see Ward[7], for instance).

The boundary conditions may be obtained by equating the velocity normal to the wing surface to zero and again equating terms of the same order in thickness, then

$$\left(\frac{\partial \phi_1}{\partial z}\right)_{z=0} = \frac{\partial z_B}{\partial x} \qquad (6)$$

$$\left(\frac{\partial \phi_2}{\partial z}\right)_{z=0} = \left(\frac{\partial z_B}{\partial x}\right)\left(\frac{\partial \phi_1}{\partial x}\right)_{z=0} + \left(\frac{\partial z_B}{\partial y}\right)\left(\frac{\partial \phi_1}{\partial y}\right)_{z=0} - z_B \left(\frac{\partial^2 \phi_1}{\partial z^2}\right)_{z=0} . \qquad \ldots (7)$$

Equations (4) and (6) correspond to the equations satisfied by thin-wing theory but general solutions of equations (5) and (7) have only been found for limiting cases such as, two-dimensional, slender, and conical wings.

The wings we are discussing here are neither two-dimensional nor very slender and it is desirable to find a method of estimating the effect of ϕ_2 on the pressure distribution. If we split ϕ_2 into two parts so that $\phi_2 = \phi_{2a} + \phi_{2b}$, then without any loss in generality we can have

$$\nabla^2 \phi_{2a} - M^2 \frac{\partial^2 \phi_{2a}}{\partial x^2} = M^2 \frac{\partial}{\partial x} (\nabla \phi_1)^2 + (\gamma - 1) M^2 \frac{\partial \phi_1}{\partial x} \nabla^2 \phi_1 \quad , \qquad (8)$$

$$\nabla^2 \phi_{2b} - M^2 \frac{\partial^2 \phi_{2b}}{\partial x^2} = 0 \quad , \qquad (9)$$

with the boundary conditions

$$\left(\frac{\partial \phi_{2a}}{\partial z}\right)_{z=0} = \frac{\partial z_B}{\partial x}\left(\frac{\partial \phi_1}{\partial x}\right)_{z=0} \qquad (10)$$

$$\left(\frac{\partial \phi_{2b}}{\partial z}\right)_{z=0} = \frac{\partial z_B}{\partial y}\left(\frac{\partial \phi_1}{\partial y}\right)_{z=0} - z_B\left(\frac{\partial^2 \phi_1}{\partial z^2}\right)_{z=0} . \qquad (11)$$

The solution of the equations for ϕ_{2b} may be obtained from the methods available for thin-wing theory since the differential equation (equation (9)) is the same. The only difficulty is that the boundary condition (equation (11)) has logarithmic singularities at the leading edge of the wing unless the first-order solution is made uniformly valid.

The solution of equations (8) and (10) for ϕ_{2a} is, in general, not easily obtained, but may be obtained in two limiting cases. Firstly, when the slender approximation applies and ϕ_{2a} and its derivatives are small compared with ϕ_{2b} and its derivatives and, secondly, when the wing is two-dimensional the solution is obtainable and has been derived in Appendix 1.

The second-order approximation to Bernoulli's equation is

$$C_p = -2\frac{\partial \phi_1}{\partial x} - 2\frac{\partial \phi_{2a}}{\partial x} - 2\frac{\partial \phi_{2b}}{\partial x} + \beta^2\left(\frac{\partial \phi_1}{\partial x}\right)^2 - \left(\frac{\partial \phi_1}{\partial y}\right)^2 - \left(\frac{\partial \phi_1}{\partial z}\right)^2 , \qquad \ldots (12)$$

and hence the only second-order corrections to the velocity perturbations that are important in calculating the pressure coefficient are $\frac{\partial \phi_{2a}}{\partial x}$ and $\frac{\partial \phi_{2b}}{\partial x}$.

In Appendix 1 it is shown that

$$\left(\frac{\partial \phi_{2a}}{\partial x}\right)_{z=0} = \left[\frac{1}{\beta^2} - \frac{M^4(\gamma+1)}{4\beta^4}\right]\left(\frac{dz_B}{dx}\right)^2 \qquad (13)$$

for a two-dimensional wing. This solution may not, as it stands, be extrapolated to wings of other planforms since it is not compatible with the slender approximation, in which, $\left(\frac{\partial \phi_{2a}}{\partial x}\right)_{z=0}$ may be neglected compared with other second-

order thickness terms. If, however, equation (13) is rewritten in terms of $\left(\frac{\partial \phi_1}{\partial x}\right)_{z=0}$, then we have

$$\left(\frac{\partial \phi_{2a}}{\partial x}\right)_{z=0} = \left[1 - \frac{M^4(\gamma+1)}{4\beta^2}\right]\left(\frac{\partial \phi_1}{\partial x}\right)^2_{z=0} \tag{14}$$

which is acceptable for both cases since for the slender approximation case it may be neglected compared with the other second-order terms in the pressure equation. Equation (14) provides an 'interpolation' between the two-dimensional approximation and the slender approximation. Others are possible, but this is the simplest. Its use can only be justified by comparison with more exact theories and experimental results, as discussed in Section 6.

The solution of equations (9) and (11) for ϕ_{2b} has not been calculated, but the slender-theory approximation to it is readily obtained from Cooke[8], as shown in Appendix 2.

Cooke gives a result for $\Delta\varphi$, the difference in potential in changing from slender thin-wing theory to slender not-so-thin-wing theory, computed at the wing surface. His result for a wing with doubly symmetrical cross-sections at zero lift is

$$\Delta\varphi = z_B \frac{\partial z_B}{\partial x} + \left(z_B \left(\frac{\partial z_B}{\partial x}\right)_c\right)_c \tag{15}$$

where

$$\left(f(x)\right)_c = -\frac{1}{\pi}\int_{-1}^{+1} \frac{f(x')}{x - x'}\, dx' \quad . \tag{16}$$

It is shown in Appendix 2 that

$$\left(\frac{\partial \phi_{2b}}{\partial x}\right)_{z=0} = \frac{\partial \Delta\varphi}{\partial x} - \left(\frac{\partial z_B}{\partial x}\right)^2 - z_B \frac{\partial^2 z_B}{\partial x^2} \quad . \tag{17}$$

From this, equations (6), (12) and (14) and the expansion $\frac{\partial \phi_1}{\partial x} = \left(\frac{\partial \phi_1}{\partial x}\right)_{z=0} + z_B \left(\frac{\partial^2 \phi_1}{\partial x \partial z}\right)_{z=0} + \ldots$ we get

$$C_p = -2\left(\frac{\partial\phi_1}{\partial x}\right)_{z=0} - 2\frac{\partial\Delta\varphi}{\partial x} + \left[\frac{M^4(\gamma+1)}{2\beta^2} + M^2 - 3\right]\left(\frac{\partial\phi_1}{\partial x}\right)^2 - \left(\frac{\partial\phi_1}{\partial y}\right)^2 + \left(\frac{\partial z_B}{\partial x}\right)^2 \quad \ldots (18)$$

for the pressure coefficient on the surface of the wing. This result agrees with that obtained by Cooke apart from the term in $\left(\frac{\partial\phi_1}{\partial x}\right)^2$, which is negligible in the slender approximation.

An objection to the procedure used to obtain equation (18) is the lack of uniqueness in the choice of boundary conditions (10) and (11) to be satisfied by the separate parts of ϕ_2. This objection arises only because equations (8) and (9) have been treated approximately and it is weakened to the extent that the approximations are valid. The choices made were dictated by the availability of the approximate solutions used. The usefulness of equation (18) as an improvement on thin-wing theory must rest on comparisons with solutions exact to second order and with measurements in a real fluid, such as those presented in the following section.

6 DISCUSSION

One of the main purposes of these tests was to show whether the thin-wing theory may be relied upon to give the pressure distribution on a slender wing even when the thickness distribution is likely to give rise to a marked adverse pressure gradient and a large suction near the trailing edge. The results in Figs.4(a) - (d) show that, as for less extreme thickness distributions such as the 'Newby' wing (Fig.6) and the 'Lord V' wing (Fig.7), thin-wing theory works fairly well except at M = 1·4 near the trailing edge.

The measurements have been made at several Reynolds numbers, but the results have been found to be insensitive to Reynolds number provided it is greater than 5×10^6 based on the wing length. At this Reynolds number azobenzene sublimation and oil flow techniques indicate that the boundary layer is non-laminar* ahead of all the pressure points. Schlieren photographs are presented in Figs.5(a) - (d) at the highest Reynolds number at which tests were made for each Mach number. These suggest that the boundary layer has thickened considerably along the chord at all Mach numbers. But oil flow and hand shadowgraph techniques showed that the boundary layer did not separate (i.e. no reverse flow in oil flow), and that the shockwave stems from the trailing edge, or a point very close to it, at all test Mach numbers above M = 1·4. At these relatively high Reynolds numbers the Schlieren system was extremely sensitive to very small disturbances; for example, there was a slight surface imperfection at about 70% of the wing length where the surface changed from araldite to steel, this was insufficient to cause transition when the

---

*i.e. in a transitional state or truly turbulent.

boundary layer was laminar in that region but produced an apparently large disturbance on the Schlieren photograph. At M = 1·4 $\left(\frac{\beta s}{c_o} = 0{\cdot}245\right)$ Fig.5(d) a photograph is presented of the flow at a lower Reynolds number also, since this was the only instance when there was a visible difference in the flow as the Reynolds number was changed. The terminal shock-wave appears to have moved forward from the wing trailing edge* at the higher Reynolds numbers and its location depends on Reynolds number. In fact the pressure measurements (Fig.4(d)) confirm that the recompression has moved forward over the central region since there is a marked drop in suction near the trailing edge for the higher Reynolds numbers; the measurements at y/s = 0·5 show no such change with Reynolds number.

In a normal two-dimensional compression corner with no upstream pressure gradient, separation moves downstream as the Reynolds number increased[10]. This suggests that some further mechanism is involved in the present case. In fact, the calculated local Mach number on the centre line at the trailing edge at a free stream Mach number of 1·4 is close to that at which the turning of the flow from the wing surface into the free stream direction can no longer be achieved through an oblique shock.

Cooke[11] has investigated the influence of a turbulent boundary layer on the pressure distribution for delta wings at zero lift. His examples are, wing 3 at $\frac{\beta s}{c_o} = 0{\cdot}487$ (Fig.4(a)), and the 'Lord V' wing at $\frac{\beta s}{c_o} = 0{\cdot}577$ (Fig.7), from which he concluded that the increment of pressure due to the boundary layer is relatively small, and is not sufficient to account for the differences found between the experimental and theoretical results. In fact, the actual magnitude of the calculated pressure increment does not exceed 0·002 at a Reynolds number of 10^7, over most of the region where pressures have been measured.

The results of slender thin-wing theory have also been plotted in Figs.4(a) - (d) and they indicate how misleading slender theory results may become when the condition of slenderness is violated. In fact on the rear part of any slender wing unless the pressure gradients are extremely small it can only be fortuitous if the slender theory is accurate since the slenderness condition is $\beta^2|\phi_{xx}| \ll |\phi_{yy}| + |\phi_{zz}|$ and the right hand side is small.

In Section 5.2 an attempt was made to formulate a not-so-thin-wing theory for pressure coefficients by estimating the terms that were not known to second-order accuracy by the most accurate available method. This method is similar to that formulated by Cooke[8], who obtains all the second order terms from the slender approximation. His method worked quite well

---

*This result was confirmed by tests on the same model at lower supersonic speeds in the R.A.E. 2' × 1½' Transonic Tunnel[9].

for the Lord V and Newby wings where slender theories are known to give reasonable results, but he found that it failed to give any improvement over thin-wing theory for the measurements described here. This is perhaps not surprising since the slenderness assumption is violated for this wing.

The results of the not-so-thin-wing theory are most encouraging since the method shows a marked improvement over thin-wing theory for the 'Newby' wing (Fig.6) and the 'Lord V' wing (Fig.7), both near the centre line and further out on the span. The method also shows a slight improvement for these wings over Cooke's method (results not shown) especially away from the centre-line where his method failed to give much improvement over thin-wing theory. On Figs.6 and 7 other curves are included with certain of the second-order terms equated to zero in order that the influence of the various terms in equation (4) may be appreciated. The results for $\phi_2 = 0^*$, $z = 0$ is what would be obtained if the boundary conditions were applied at $z = 0$ and the pressure computed in that plane and the $\phi_{2b} = 0$, $z = 0$ indicates the change in pressure coefficient on including the estimate for $\left(\frac{\partial \phi_{2a}}{\partial x}\right)$. At $y/s = 0{\cdot}4$ the curve for $\phi_2 = 0$, $z = 0$ has been omitted since it is very nearly the same as the curve for thin-wing theory. From these results it appears that both $\left(\frac{\partial \phi_{2a}}{\partial x}\right)_{z=z_B}$ and $\left(\frac{\partial \phi_{2b}}{\partial x}\right)_{z=z_B}$ may be appreciable and that the proposed methods of estimation work quite well for both these wings. The method has also been used to estimate the pressure coefficients for wing 3 (Figs.4(a) - (d)) and the results show a marked improvement at all test Mach numbers over thin-wing theory especially near the centre line. The improvement is perhaps surprising since $\left(\frac{\partial \phi_{2b}}{\partial x}\right)_{z=z_B}$ is obtained from slender theory and the slenderness assumption is known to be violated for this wing. At the $y/s = 0{\cdot}5$ station there is a tendency for the pressure to be higher than that estimated, especially where the surface slope is small.

In all cases where the not-so-thin-wing theory has been tried for delta wings there has been a marked improvement over thin-wing theory for the pressure distribution. The programme mentioned previously for the computation of the thin-wing theory pressure coefficients[5] has been adapted to give results for the not-so-thin-wing theory method. The method is equally applicable to more complicated planforms and thickness distributions, and, provided the first order perturbation velocity components are known, can be simply applied since the method involves only the first-order perturbation velocity components and a thickness correction from slender theory.

A further check on the method is possible by considering the pressure distribution on a conical body of rhombic cross-section (Fig.8) since for this example a full second-order solution exists[12,13] as well as some measurements

---

* $\phi_2 = \phi_{2a} + \phi_{2b}$

made at R.A.E. Bedford[14,15,16]. The experimental results presented here have in fact been extracted from Küchemann's[16] paper, where he shows that slender-body theory and thin-wing theory are never fully adequate. The present method predicts almost the same variation in pressure coefficient with Mach number as the full second-order theory but it tends to overestimate the pressure coefficient. As anticipated, the method fails near the wing leading edge. Lighthill[17], Van Dyke[18], Randall[19] and Weber[20] have shown how the predictions of thin-wing theories near leading edges can be improved and such techniques could be combined with the present method. The full second order results show remarkably good agreement with the experimental results.

The present method is not suitable for computing the wave drag since the theory gives a non-integrable singularity near the wing leading edge.

7 CONCLUSIONS

The results presented in the preceding sections suggest that small-perturbation methods taken to second-order accuracy, but with certain of the terms estimated by cruder methods, may be used to predict the pressure coefficients, on slender delta wings of rhombic cross-sections at zero lift, at points not too close to the wing leading edge, even for a wing with an adverse pressure gradient over part of the chord and a relatively large suction near the trailing edge. The method suggested is relatively simple to apply, and it is recommended that it should be tried on other planforms and cross sections.

Slender theory should not be relied upon for the calculation of the pressure coefficients since in the region of the trailing edge the assumption of slenderness $\{\beta^2|\phi_{xx}| << |\phi_{yy}| + |\phi_{zz}|\}$ is valid only for a very restricted range of wings. Thin-wing theory on the other hand gives quite a good first approximation to the pressure coefficient in all cases tried.

The experimental results indicate that the trailing-edge shock wave may, depending on thickness distribution, still be detached from the trailing edge at Mach numbers as high as 1·4 without any positive signs of boundary-layer separation. Further work is necessary if the transonic behaviour of the trailing-edge shock wave is to be understood.

SYMBOLS

C_p = pressure coefficient $\left(\frac{p - p_\infty}{q}\right)$

ΔC_p = change in pressure coefficient due to thickness (see Section 4.2)

c_o = wing chord at centre line

F_1, F_2, G_1, G_2 = arbitrary functions

f_c = conjugate of f i.e. $-\frac{1}{\pi}\int_{-1}^{+1} \frac{f(x')\ dx'}{x - x'}$

K_o = zero lift wave drag factor

p = local pressure

p_∞ = ambient pressure

q = kinetic pressure of free stream

M = mean free stream Mach number

Re = Reynolds number based on wing chord at centre line

s = semi-span at the trailing edge

t = max wing thickness

$S(\xi)$ = cross-sectional area in plane normal to free stream

V = volume of the wing

x, y, z = Cartesian coordinates with origin at the apex of the wing; x axis measured in the direction of the undisturbed stream; the z axis normal to the chordal plane of the wing

z_B = z ordinate of the wing surface

β = $\sqrt{M^2 - 1}$

ξ = x/c_o, the chordwise station as a fraction of the centre line chord and measured from the apex

SYMBOLS (Contd)

ϕ	=	velocity potential
ϕ_1	=	1st order velocity potential perturbation
ϕ_2	=	2nd order correction to ϕ_1
ϕ_{2a}, ϕ_{2b}	=	see Section 5.2
$\Delta\varphi$	=	change in velocity potential between a thin wing and a body theory (see Section 5.2)
τ	=	$v/(\text{planform area})^{3/2}$, a volume parameter

REFERENCES

No.	Author	Title, etc
1	Firmin, M.C.P.	Experimental evidence on the drag at zero lift on a series of slender delta wings at supersonic speeds and the drag penalty due to distributed roughness. A.R.C. C.P. 737. February 1963.
2	Midwood, G.F., Hayward, R.W.	An automatic self-balancing capsule manometer. A.R.C. C.P.231. July, 1955.
3	Eminton, E.	Pressure distributions at zero-lift for delta wings with rhombic cross-sections. A.R.C. C.P.525. October, 1959.
4	Smith, J.H.B., Beasley, J.A., Short, D., Walkden, F.	The calculation of the warp to produce a given load and the pressures due to a given thickness on thin slender wings in supersonic flow. Unpublished M.O.A. Report.
5	Firmin, M.C.P.	A programme for the computation of pressures on delta wings of rhombic cross-sections at supersonic speeds. Unpublished M.O.A. Report.
6	Weber, J.	Slender delta wings with sharp edges at zero lift. A.R.C. 19,549. May 1957.

REFERENCES (Contd)

No.	Author	Title, etc
7	Ward, G.N.	Linearized theory of steady high speed flow. Cambridge Monograph on Mechanics and Applied Mathematics. C.U.P. 1955.
8	Cooke, J.C.	Slender not-so-thin wing theory. A.R.C. C.P.659. January 1962.
9	Firmin, M.C.P.	Flow visualization and pressure distribution on a slender delta wing of diamond section at transonic speeds. Unpublished M.O.A. Report.
10	Eminton, E.	Simple theoretical and experimental studies of the flow through a three-shock system in a corner. A.R.C. C.P.727. September 1961.
11	Cooke, J.C.	Turbulent boundary layers on delta wings at zero lift. A.R.C. C.P.696. March 1963.
12	Fenain, M., Germain, P.	Sur la résolution de l'équation régissants en seconde approximation, les écoulements d'un fluide autour d'obstacles tridimensionnels. Cromptes Rendus de l'Académie des Sciences, Vol.241, page 276. 1955.
13	Fenain, M.	Numerical values for F_i in Comptes Rendus de l'Académie des Sciences, Vol.241, page 276. (Private communication)
14	Britton, J.W.	Pressure measurements at supersonic speeds on three uncambered conical wings of unit aspect ratio. A.R.C. C.P.641. May 1962.
15	Squire, L.C.	Pressure distributions and flow patterns on some conical shapes with sharp edges and symmetrical cross sections at M = 4·0. A.R.C. R & M 3340. June, 1962.
16	Küchemann, D.	On some three-dimensional flow phenomena of the transonic type. IOTAM Symposium Transonicum Anchen. A.R.C. 24,311. 1962.
17	Lighthill, M.J.	A new approach to thin aerofoil theory. Aero Quart. Vol.3, page 193. 1951.

REFERENCES (Contd)

No.	Author	Title, etc
18	Van Dyke, M.D.	Subsonic edges in thin-wing and slender body theory. NACA TN 3343. November 1954.
19	Randall, D.G.	An improvement of the velocity distribution predicted by linear theory for wings with straight subsonic leading edges. A.R.C. C.P.418. September 1958.
20	Weber, J.	Rendering the slender thin-wing theory for symmetrical wings with sharp edges uniformly valid. Unpublished M.O.A. Report.

APPENDIX 1

DETERMINATION OF THE SECOND ORDER SOLUTION TO THE POTENTIAL EQUATION FOR TWO DIMENSIONAL FLOW

In two dimensions equation (4) may be written as

$$\beta^2 \frac{\partial^2 \phi_1}{\partial x^2} - \frac{\partial^2 \phi_1}{\partial z^2} = 0 \qquad (19)$$

the general solution of which is

$$\phi_1 = G_1(x - \beta z) + G_2(x + \beta z) \qquad (20)$$

where G_1 and G_2 are arbitrary functions. The boundary conditions for ϕ_1 are

$$\phi_1 = 0 \quad \text{for} \quad x - \beta z < 0 \quad \text{and} \quad \left(\frac{\partial \phi_1}{\partial z}\right)_{z=0} = \frac{dz_B}{dx} = f(x) \text{ (say)}$$

from which we may obtain

$$\frac{\partial \phi_1}{\partial x} = -\frac{1}{\beta} f(x - \beta z), \quad \frac{\partial \phi_1}{\partial z} = f(x - \beta z) \qquad (21)$$

which satisfy the boundary conditions at $z = 0$.

Having obtained a general solution to equation (19) we now have enough information to solve the differential equation for ϕ_{2a} in two dimensions i.e.

$$\beta^2 \frac{\partial^2 \phi_{2a}}{\partial x^2} - \frac{\partial^2 \phi_{2a}}{\partial z^2} = -M^2 \frac{\partial}{\partial x} (\nabla \phi_1)^2 - (\gamma - 1) M^2 \frac{\partial \phi_1}{\partial x} \nabla^2 \phi_1 \ . \qquad \ldots (22)$$

On substituting the first order solutions from equations (21) we get

$$\beta^2 \frac{\partial^2 \phi_{2a}}{\partial x^2} - \frac{\partial^2 \phi_{2a}}{\partial z^2} = -\frac{M^4(\gamma+1)}{\beta^2} f(x - \beta z) f'(x - \beta z) \qquad (23)$$

with boundary conditions from equation (11).

i.e.

$$\left(\frac{\partial \phi_{2a}}{\partial z}\right)_{z=0} = \frac{dz_B}{dx}\left(\frac{\partial \phi_1}{\partial x}\right)_{z=0} = -\frac{1}{\beta}\left(\frac{dz_B}{dx}\right)^2$$

with

$$\phi_{2a} = 0 \quad \text{for} \quad x - \beta z < 0 \ . \tag{24}$$

If we transform equation (23) to (u,v) coordinates such that $u = x - \beta z$ and $v = x + \beta z$ we obtain

$$\frac{\partial^2 \phi_{2a}}{\partial u \partial v} = -\frac{M^4}{4\beta^4}(\gamma+1)\, f(u)\, f'(u) \tag{25}$$

the solution of which is

$$\phi_{2a} = -\frac{M^4}{8\beta^4}(\gamma+1)\left\{f(x-\beta z)\right\}^2 (x+\beta z) + F_1(x+\beta z) + F_2(x-\beta z) \qquad \ldots (26)$$

where F_1 and F_2 are arbitrary functions.

The differential equation for ϕ_{2b} in two dimensions i.e.

$$\beta^2 \frac{\partial^2 \phi_{2b}}{\partial x^2} - \frac{\partial^2 \phi_{2b}}{\partial z^2} = 0 \tag{27}$$

may be solved in a similar way, the solution of which is

$$\phi_{2b} = E_1(x+\beta z) + E_2(x-\beta z) \tag{28}$$

where E_1 and E_2 are arbitrary functions with boundary conditions from equation (12)

i.e.

$$\left(\frac{\partial \phi_{2b}}{\partial z}\right)_{z=0} = -z_B\left(\frac{\partial^2 \phi_1}{\partial z^2}\right)_{z=0} = z_B\,\beta\,\frac{d^2 z_B}{dx^2}$$

with

$$\phi_{2b} = 0 \quad \text{for} \quad x - \beta z < 0 \ . \tag{29}$$

Now on differentiating the solutions and applying the boundary conditions we get

$$F_1(x) = 0$$

$$F_2'(x) = \frac{M^4}{4\beta^4}(\gamma+1)\left(\frac{dz_B}{dx}\right)\left(\frac{d^2z_B}{dx^2}\right)x + \left[\frac{1}{\beta^2} - \frac{M^4}{8\beta^4}(\gamma+1)\right]\left(\frac{dz_B}{dx}\right)^2$$

$$E_1(x) = 0$$

$$E_2'(x) = -z_B\frac{d^2z_B}{dx^2} \quad . \tag{30}$$

The contribution to the pressure coefficient from ϕ_2 is dependent on $\frac{\partial\phi_2}{\partial x} = \frac{\partial\phi_{2a}}{\partial x} + \frac{\partial\phi_{2b}}{\partial x}$ and this may be obtained from equations (26), (28) and (30) i.e.

$$\frac{\partial\phi_{2a}}{\partial x} = -\frac{M^4}{4\beta^4}(\gamma+1)\,f(x-\beta z)\,f'(x-\beta z)(x+\beta z) - \frac{M^4}{8\beta^4}(\gamma+1)\{f(x-\beta z)\}^2 + F_2'(x-\beta z)$$

and

$$\frac{\partial\phi_{2b}}{\partial x} = E_2'(x-\beta z) \tag{31}$$

so that since we require only $\frac{\partial\phi_z}{\partial x}$ on the wing surface and all terms are already of second order we obtain

$$\left(\frac{\partial\phi_{2a}}{\partial x}\right)_{z=z_B} = \left[\frac{1}{\beta^2} - \frac{M^4}{4\beta^4}(\gamma+1)\right]\left(\frac{dz_B}{dx}\right)^2 ,$$

and

$$\left(\frac{\partial\phi_{2b}}{\partial x}\right)_{z=z_B} = -z_B\frac{d^2z_B}{dx^2} \quad . \tag{32}$$

Appendix 1

Although for the present application we require only $\left(\frac{\partial \phi_{2a}}{\partial x}\right)$ it is of interest to determine the pressure coefficient computed on the wing surface to second order accuracy for a two dimensional wing

i.e.

$$C_p = -2\left(\frac{\partial \phi_1}{\partial x}\right)_{z=z_B} - 2\left(\frac{\partial \phi_{2a}}{\partial x}\right)_{z=z_B} - 2\left(\frac{\partial \phi_{2b}}{\partial x}\right)_{z=z_B} \qquad (33)$$

and since

$$\left(\frac{\partial \phi_1}{\partial x}\right)_{z=z_B} = -\frac{1}{\beta} f(x-\beta z_B) = -\frac{1}{\beta}\frac{dz_B}{dx} + z_B \frac{d^2 z_B}{dx^2} + \ldots$$

we obtain

$$C_p = \frac{2}{\beta}\frac{dz_B}{dx} - \left[\frac{4\beta^2 - M^4(\gamma+1)}{2\beta^4}\right]\left(\frac{dz_B}{dx}\right)^2 + \ldots \qquad (34)$$

which agrees with the result obtained by Busemann from simple wave theory.

APPENDIX 2

DETERMINATION OF $\left(\frac{\partial \phi_{2b}}{\partial x}\right)_{z=z_B}$ FROM SLENDER THEORY IN TERMS OF THE DIFFERENCE IN POTENTIAL BETWEEN NOT-SO-THIN-WING THEORY AND THIN WING

Let $\varphi_T(x,y,z)$ be the velocity potential when obtained from slender thin wing theory and $\varphi_B(x,y,z)$ be the velocity potential when obtained from slender not-so-thin wing theory, then we may write for small z and small $(z - z_B)$,

$$\varphi_T(x,y,z) = \varphi_T(x,y,0) + z\left(\frac{\partial \varphi_T}{\partial z}\right)_{z=0} + \cdots \tag{35}$$

$$\varphi_B(x,y,z) = \varphi_B(x,y,z_B) + (z - z_B)\left(\frac{\partial \varphi_B}{\partial z}\right)_{z=z_B} + \cdots \tag{36}$$

by a Taylor expansion, where z_B is the location of the body surface above the $z = 0$ plane.

New Cooke[8] defines $\Delta\varphi$ as

$$\varphi_B(x,y,z_B) - \varphi_T(x,y,0) = \Delta\varphi \tag{37}$$

and by comparing the slender theory approximation to the equations for ϕ_{2b} with those solved by Cooke we have

$$\varphi_B(x,y,z) - \varphi_T(x,y,z) = \phi_{2b} \ . \tag{38}$$

Hence from equations (35) to (38) we have

$$\phi_{2b} = \Delta\varphi - z_B \frac{\partial z_B}{\partial x} \tag{39}$$

since $\left(\frac{\partial \varphi_T}{\partial z}\right)_{z=0}$ and $\left(\frac{\partial \varphi_B}{\partial z}\right)_{z=z_B}$ may both be replaced by $\frac{\partial z_B}{\partial x}$ to the order of accuracy required.

Appendix 2

On differentiating equation (39) with respect to x we have

$$\frac{\partial \phi_{2b}}{\partial x} = \frac{\partial}{\partial x}(\Delta\varphi) - z_B \frac{\partial^2 z_B}{\partial x^2} - \left(\frac{\partial z_B}{\partial x}\right)^2 . \qquad (40)$$

Printed in England for Her Majesty's Stationery Office by the Royal Aircraft Establishment, Farnborough. W.T.60.K.4.

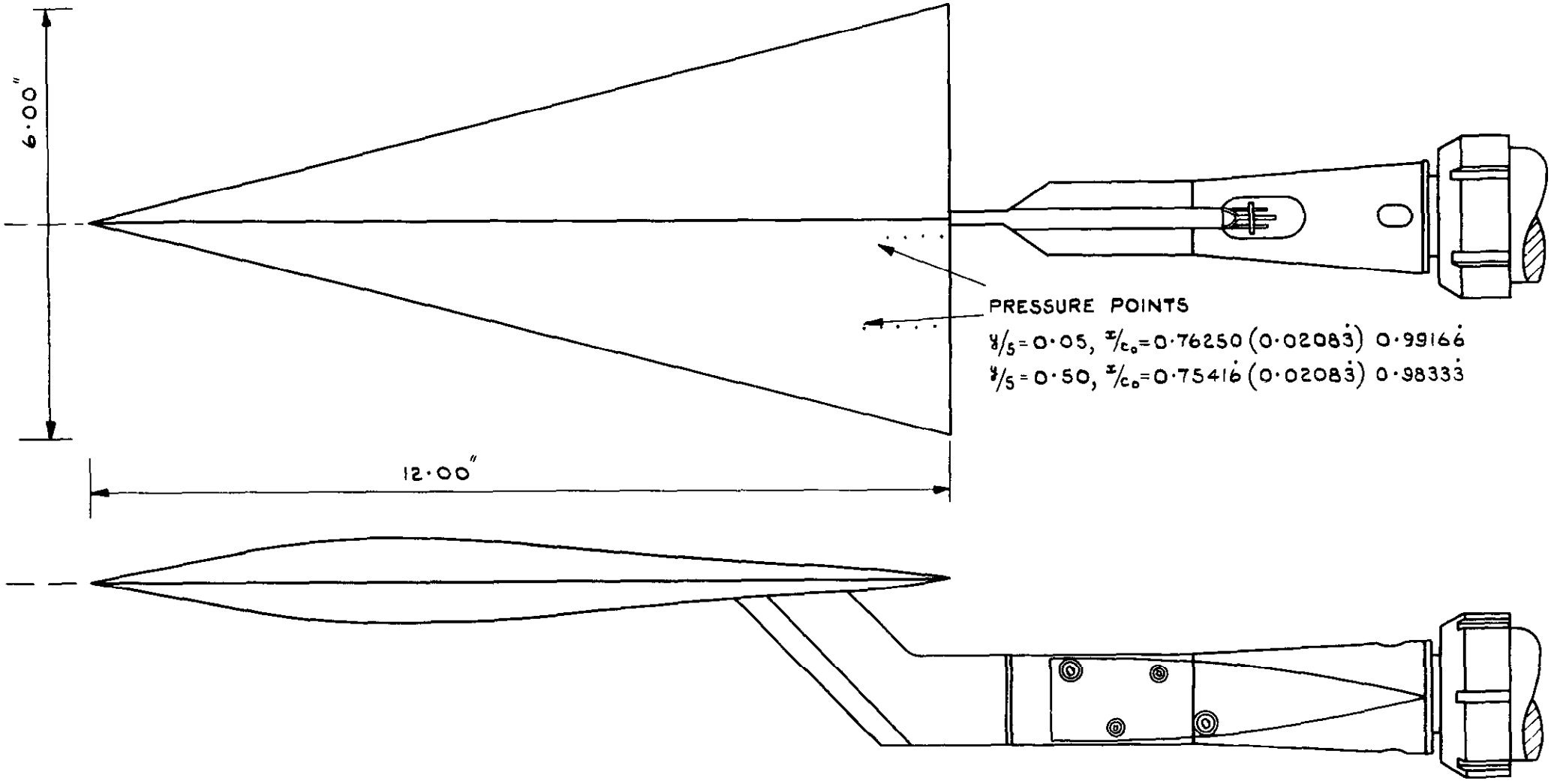

FIG 1 MODEL DETAILS (WING 3) SCALE 1/2.

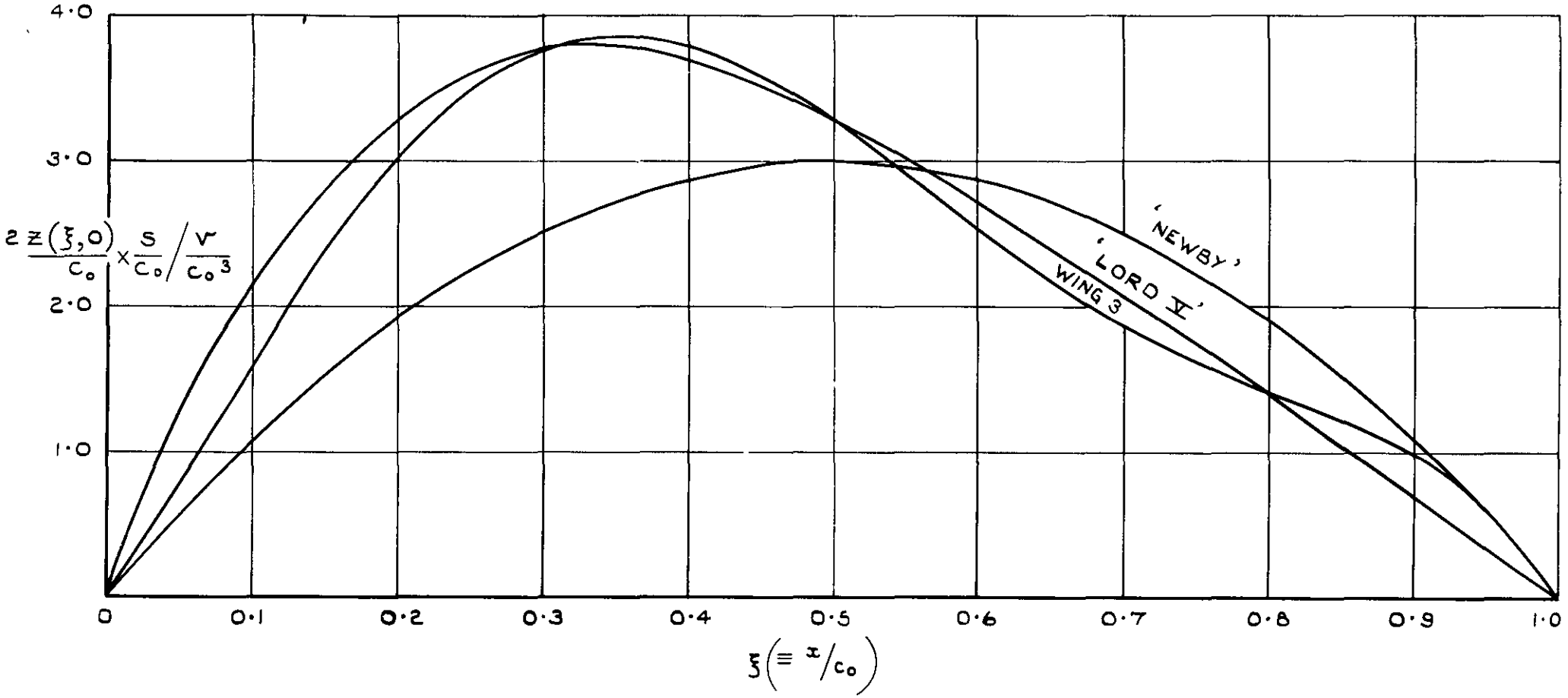

FIG. 2. NON-DIMENSIONAL CENTRE LINE THICKNESS DISTRIBUTIONS.

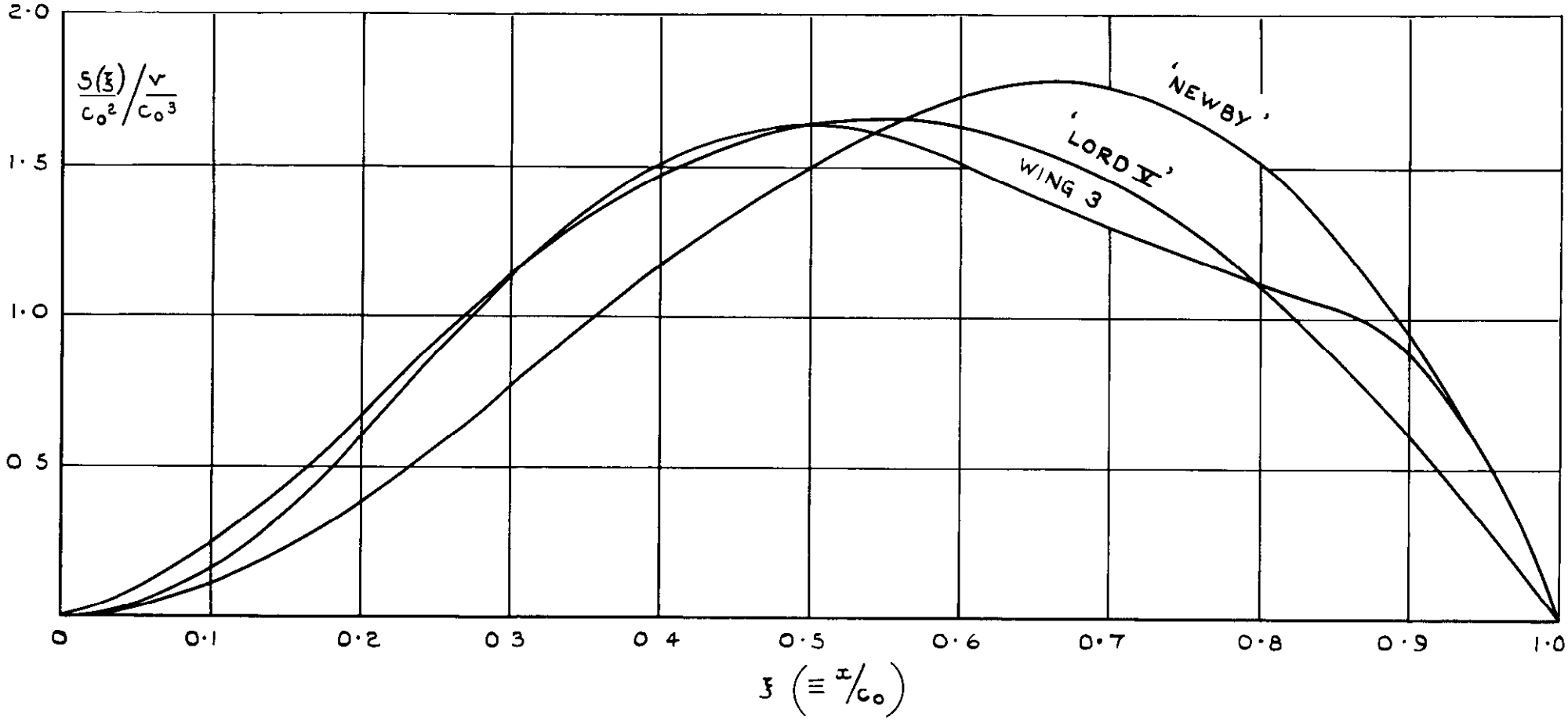

FIG.3. NON-DIMENSIONAL CROSS SECTIONAL AREA DISTRIBUTIONS.

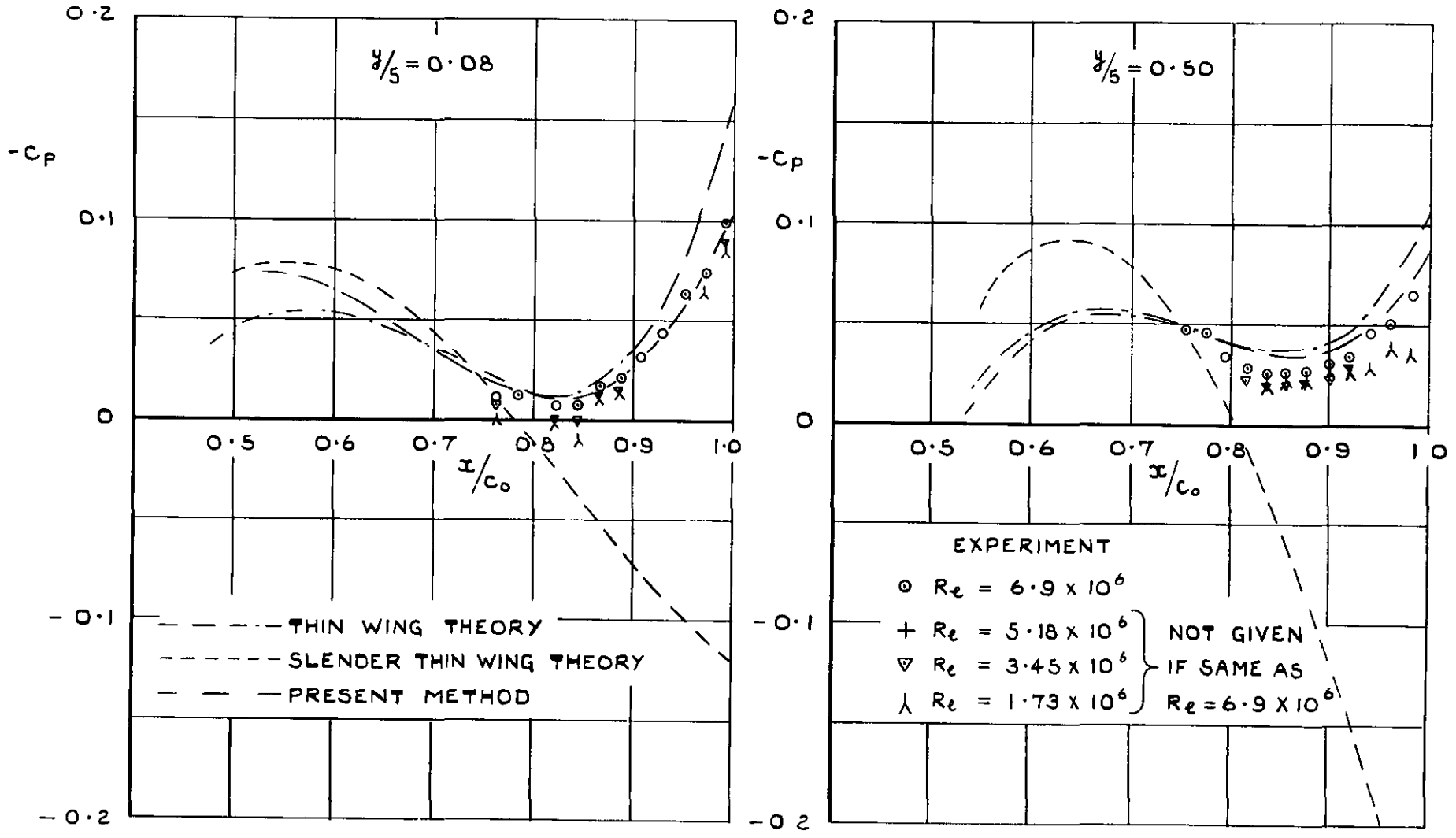

FIG. 4 (a) PRESSURE DISTRIBUTION AT M=2·19, $\beta s/c_o$=0·487—WING 3.

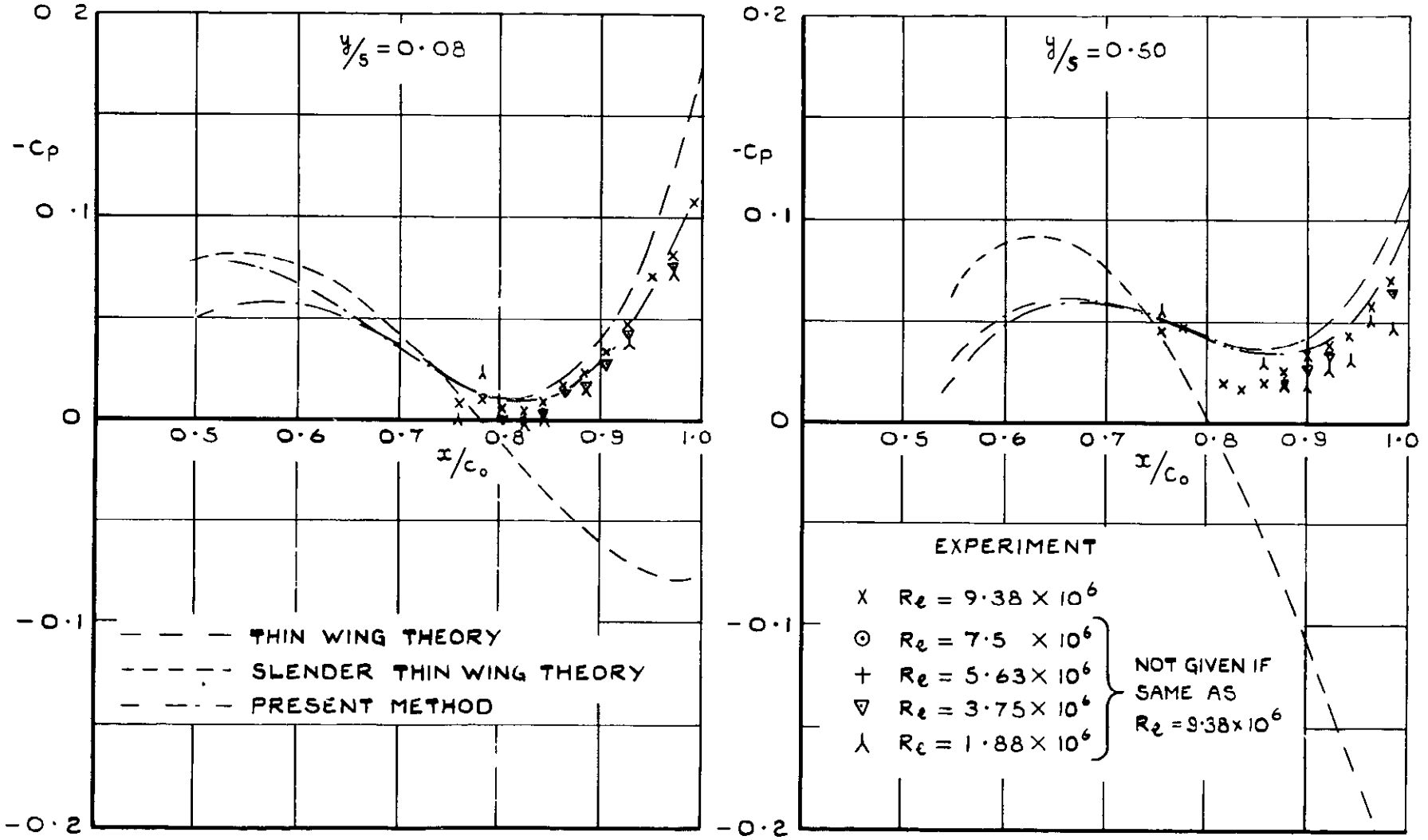

FIG 4 (b) PRESSURE DISTRIBUTION AT M=2 02, $\beta s/c_o = 0 \cdot 436$ – WING 3 .

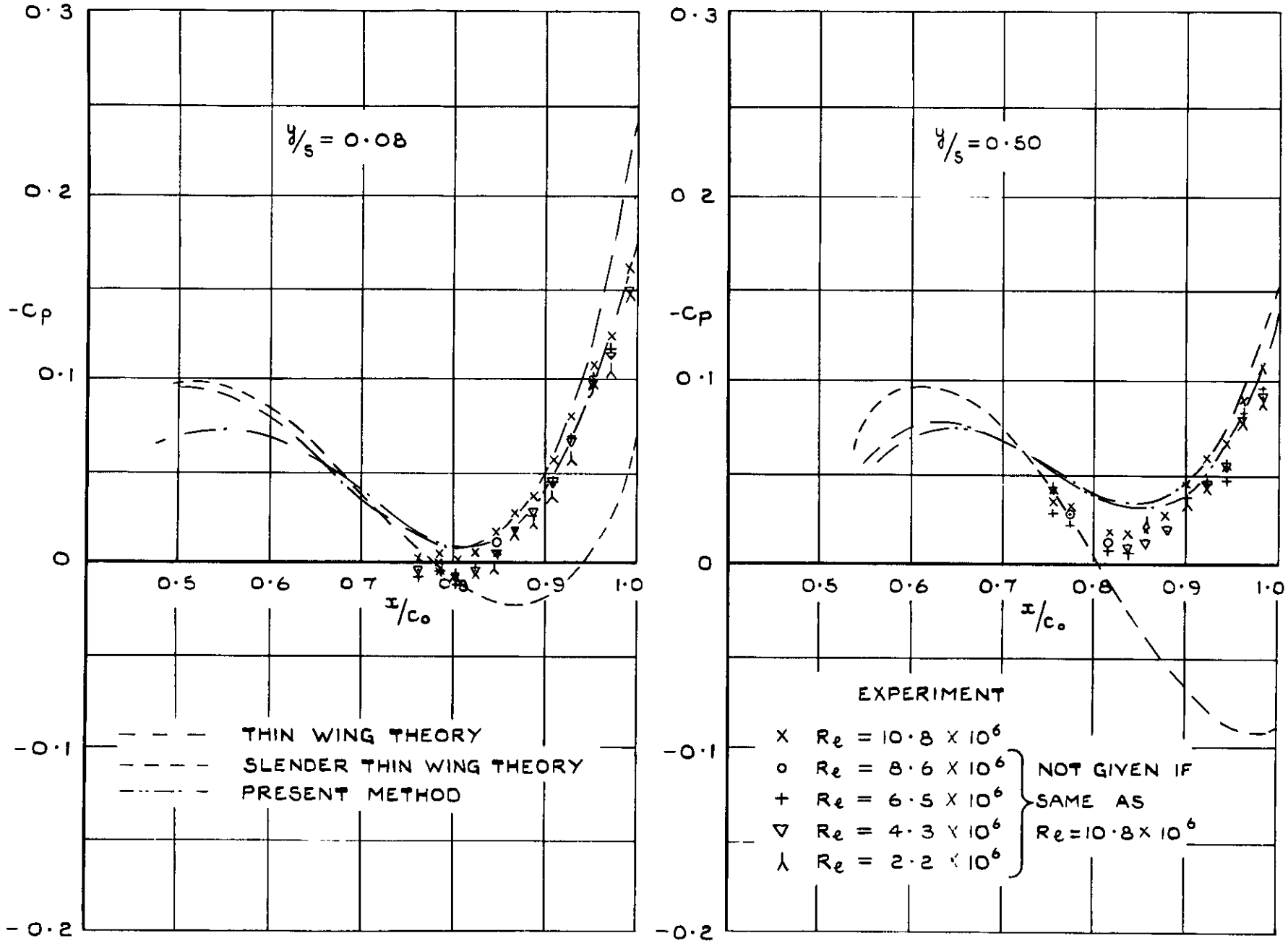

FIG. 4(c) PRESSURE DISTRIBUTION AT M = 1·58, $\beta s/c_o = 0·306$ - WING 3.

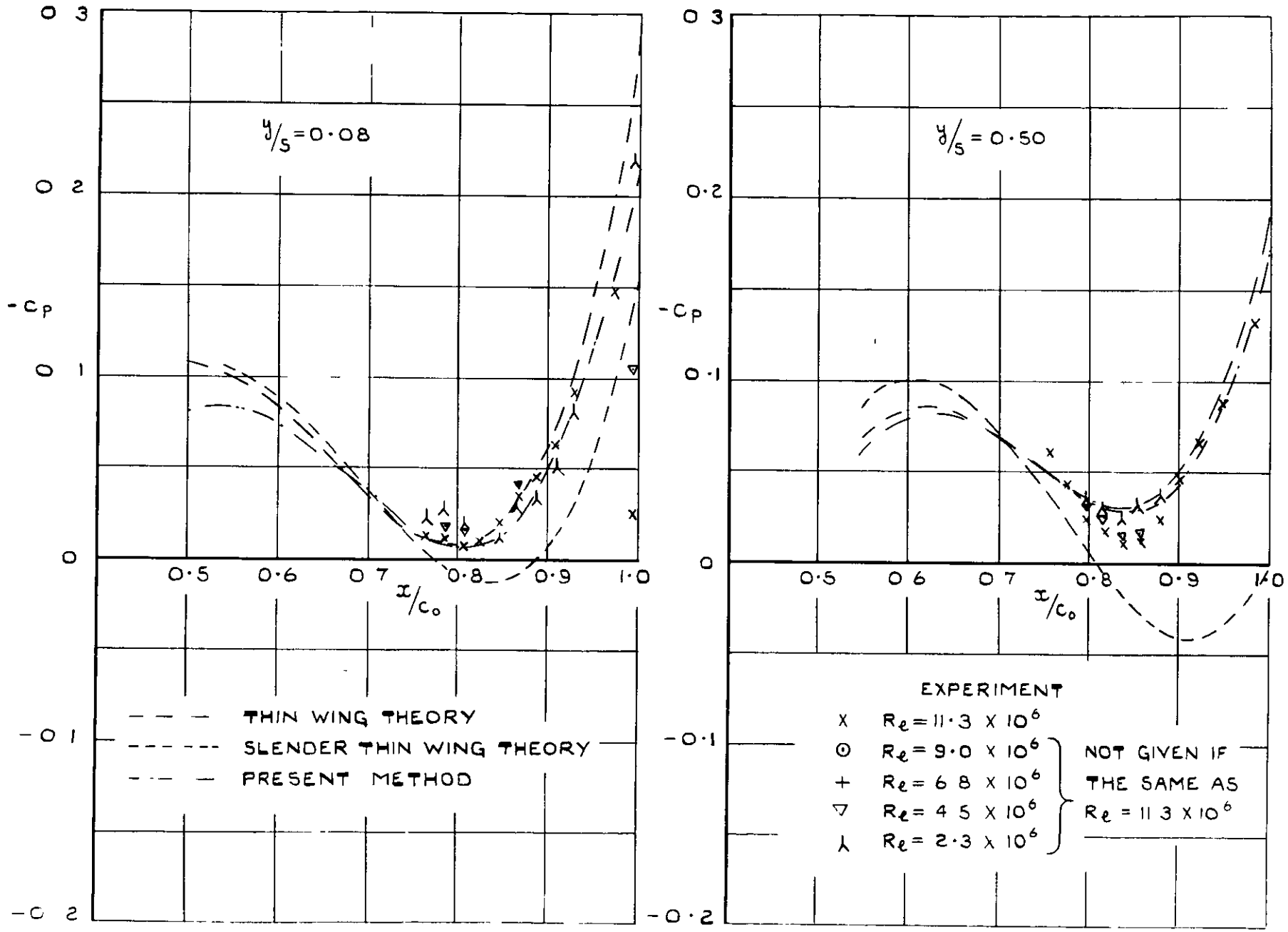

FIG. 4(d) PRESSURE DISTRIBUTION AT M = 1·4, $\beta s/c_o = 0.245$ - WING 3

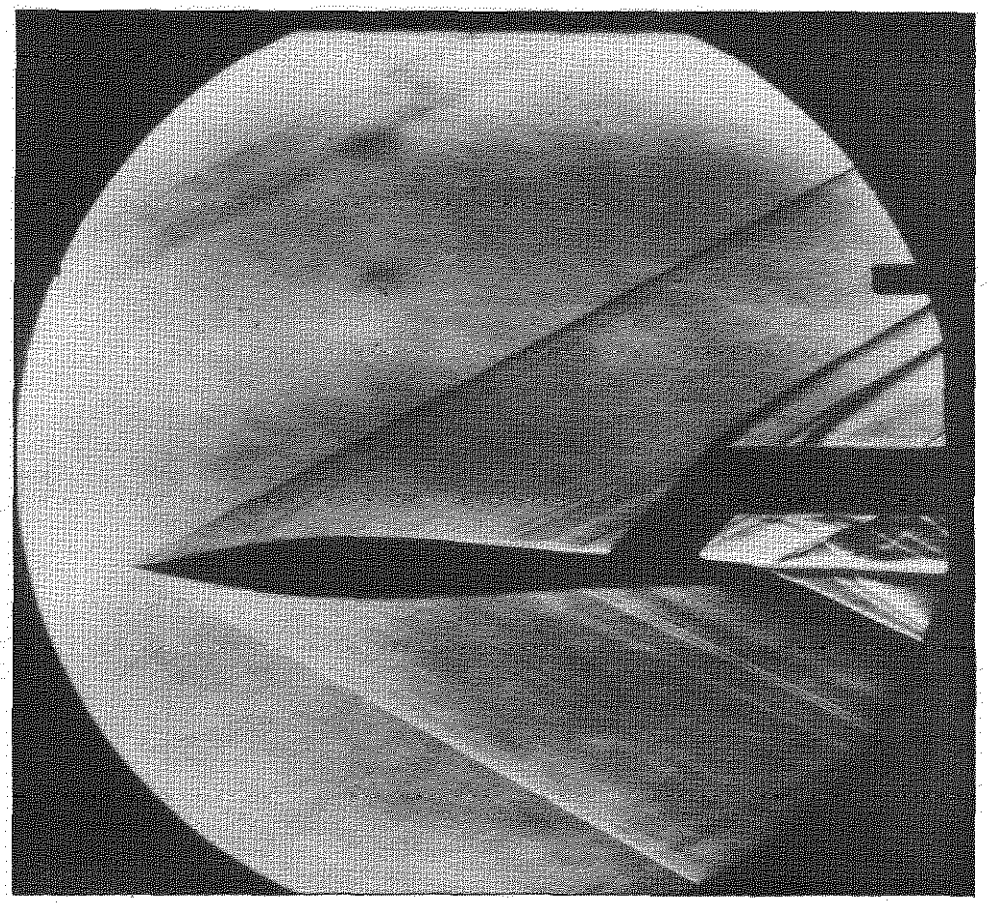

FIG.5(a) SCHLIEREN $M = 2{\cdot}19$ $Re = 6{\cdot}9 \times 10^6$ $\left(\frac{\beta s}{c} = 0{\cdot}487\right)$

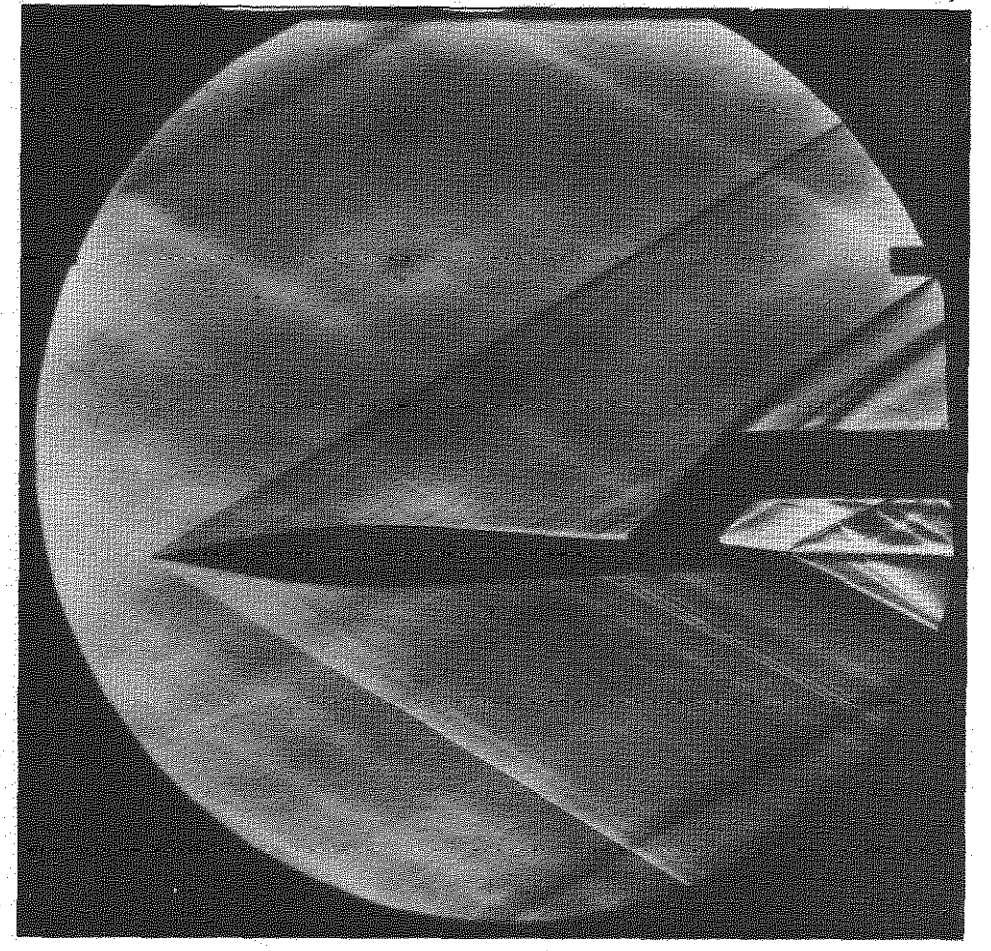

FIG.5(b) SCHLIEREN $M = 2{\cdot}02$ $\left(\frac{\beta s}{c} = 0{\cdot}439\right)$ $Re = 9{\cdot}38 \times 10^6$

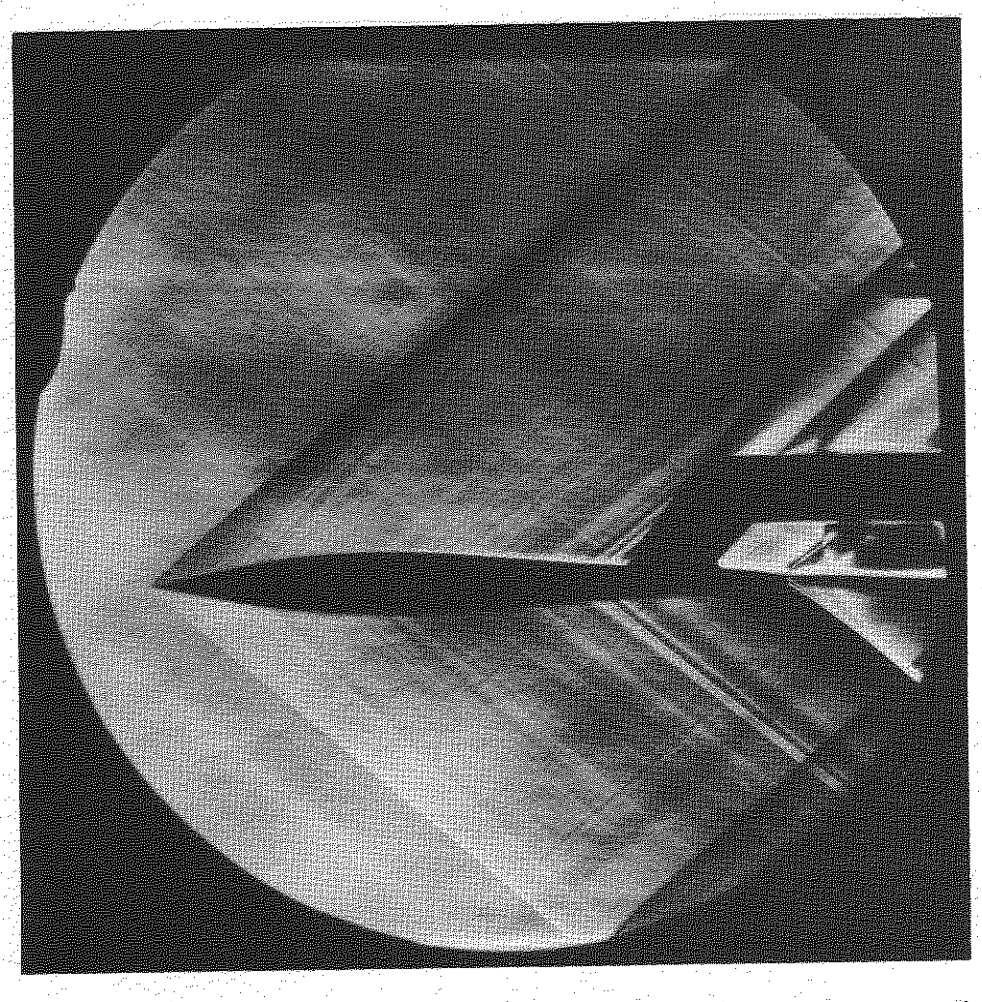

FIG.5(c) SCHLIEREN $M = 1{\cdot}58$ $\left(\frac{\beta s}{c} = 0{\cdot}306\right)$ $Re = 10{\cdot}8 \times 10^6$

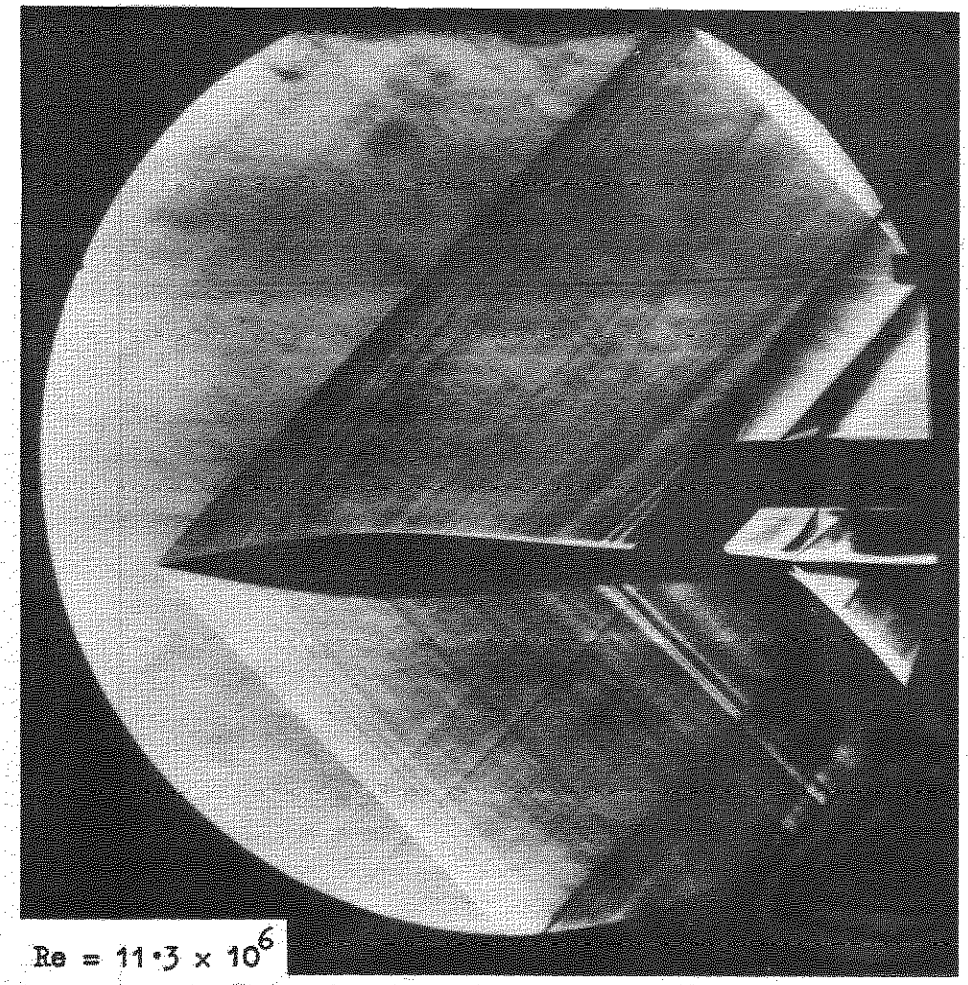

Re = $11 \cdot 3 \times 10^6$

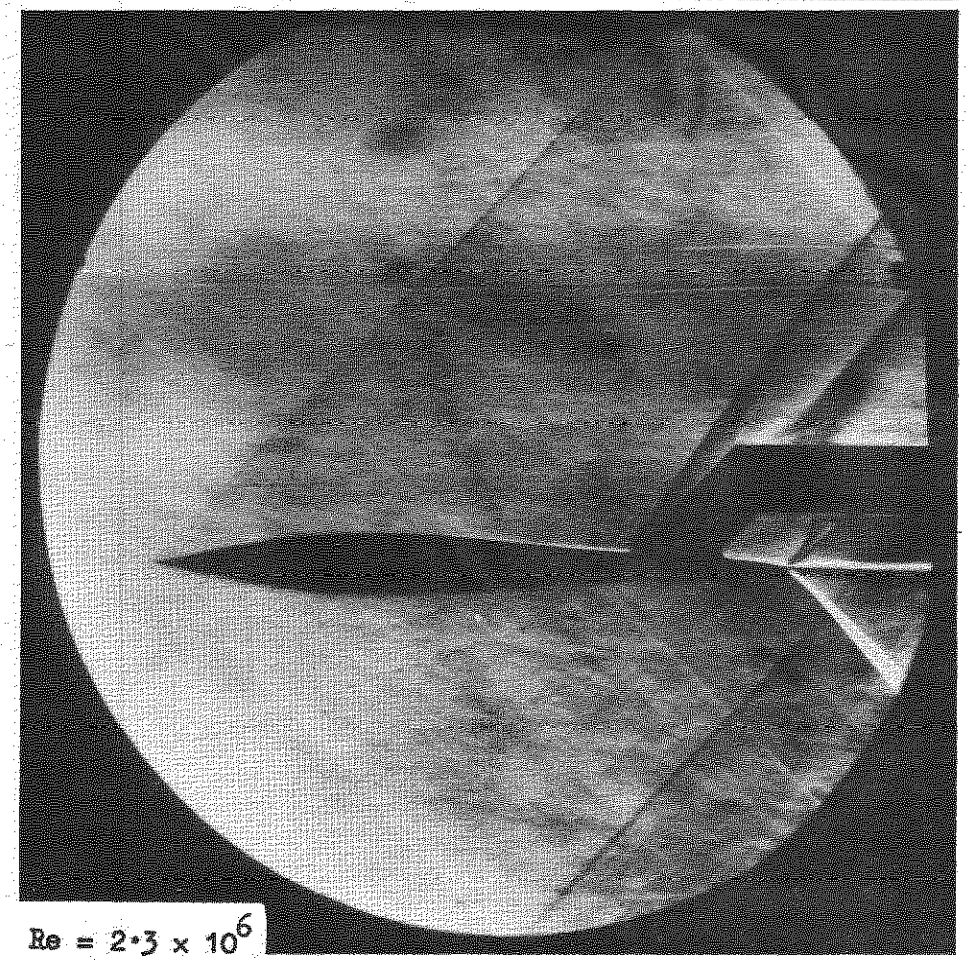

Re = $2 \cdot 3 \times 10^6$

FIG.5(d) SCHLIEREN M = 1·4 $\left(\frac{\beta s}{c} = 0 \cdot 245\right)$

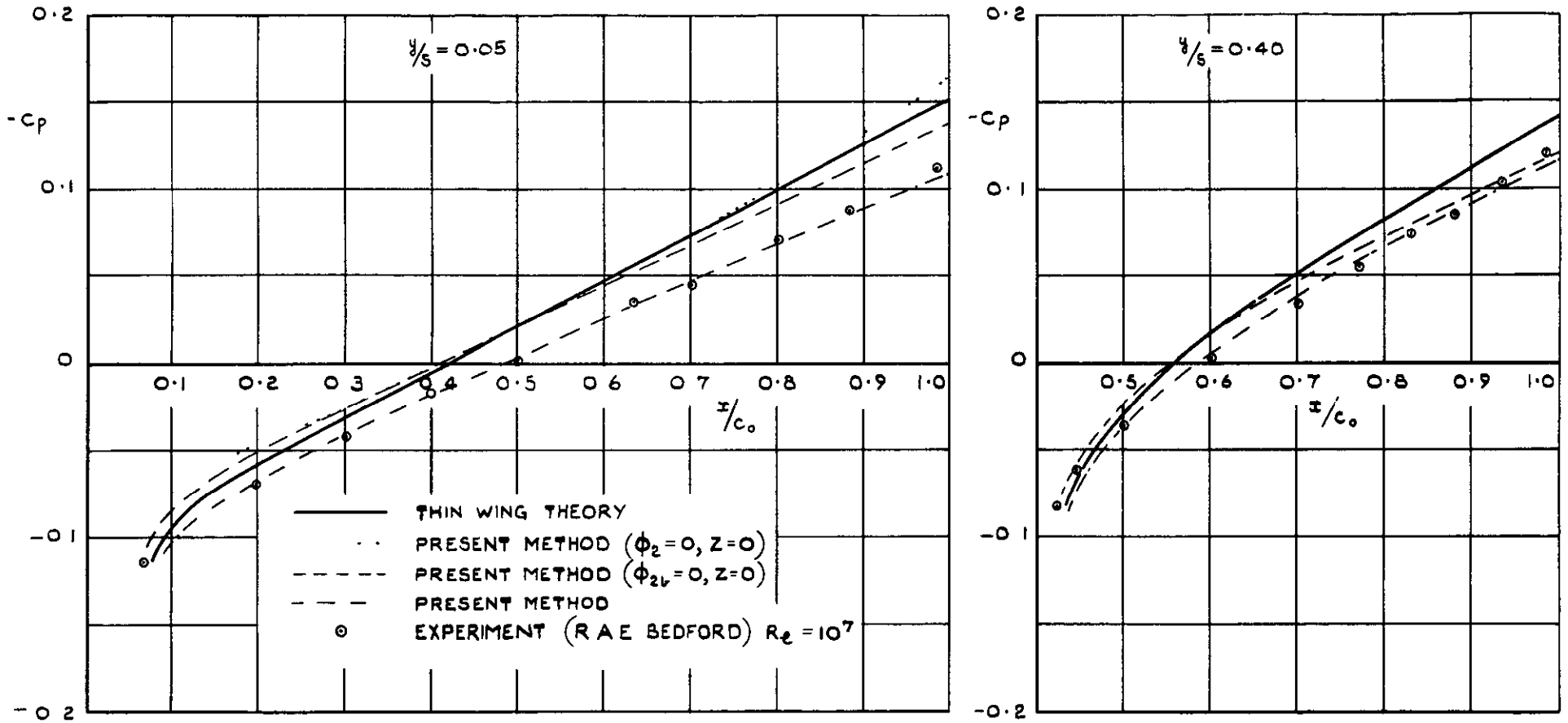

FIG. 6. PRESSURE DISTRIBUTION AT $M = 2 \cdot 0$, $\beta s/c_0 = 0 \cdot 577$ "NEWBY" WING.

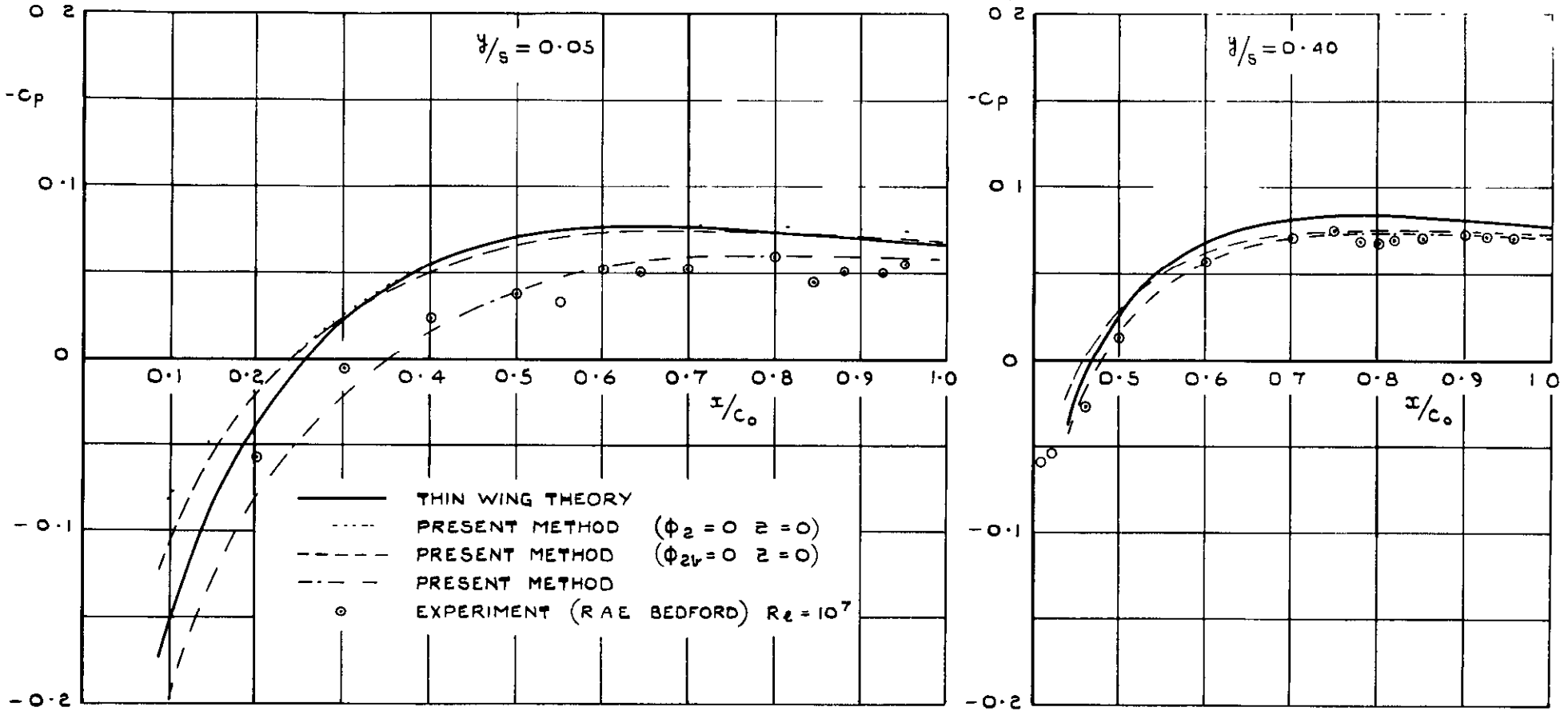

FIG.7. PRESSURE DISTRIBUTION AT M = 2·00, $\beta s/c_0 = 0{\cdot}577$ "LORD V" WING.

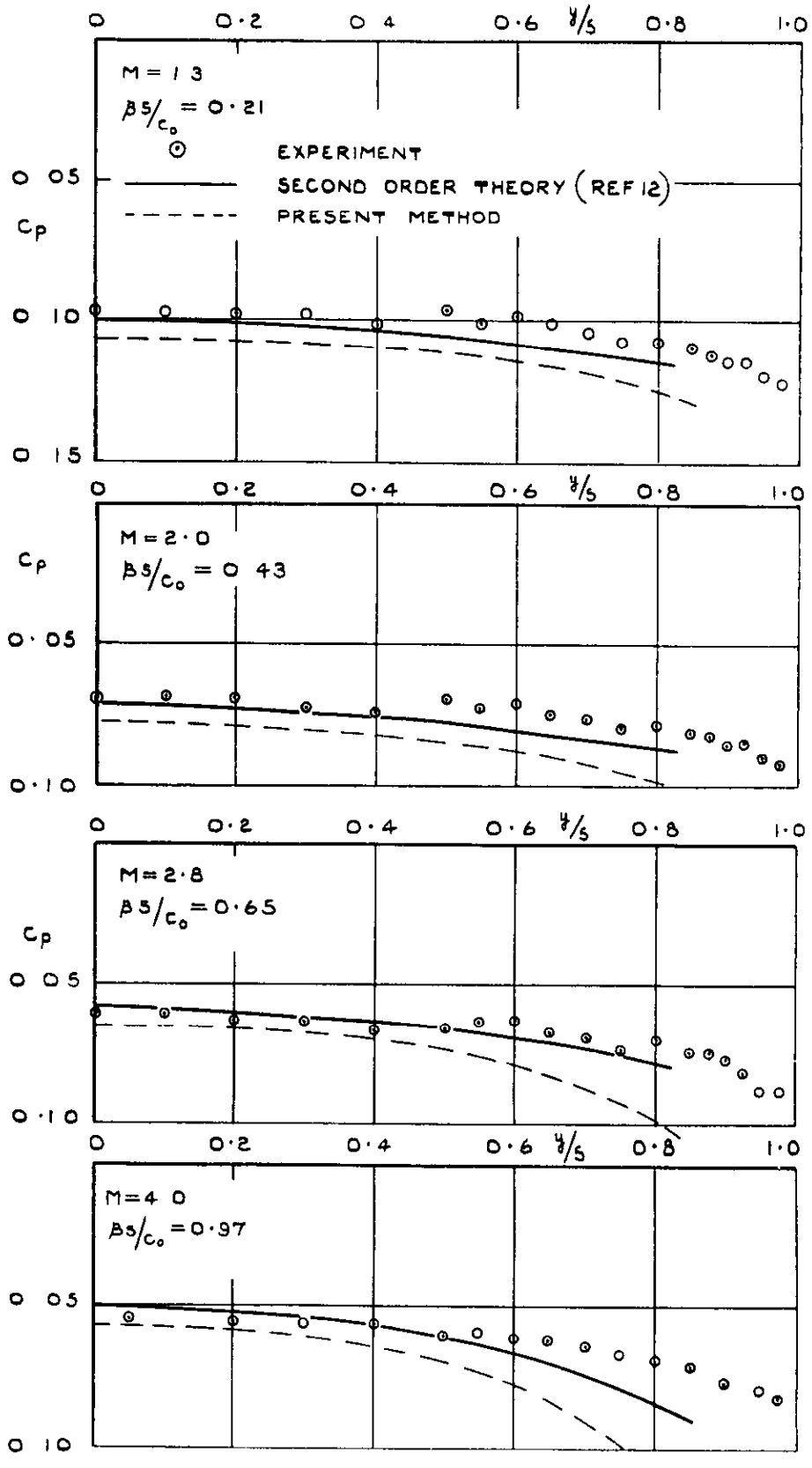

FIG. 8. PRESSURE DISTRIBUTIONS OVER A CONICAL BODY WITH RHOMBIC CROSS-SECTIONS.

$\left(s/c_0 = 0.25, \quad \tau = 0.385 \right)$

A.R.C. C.P. No.774

533.6.048.2 :
533.6.013.13 :
533.693.3 :
533.6.011.5

THE PRESSURE DISTRIBUTION AT ZERO-LIFT ON SOME SLENDER DELTA WINGS AT SUPERSONIC SPEEDS. Firmin, M. C. P.
November 1963.

The pressure distribution has been measured on the rear of a slender delta wing with rhombic cross-sections as part of a programme to investigate the influence on the wave drag of thickness distributions that give rise to a marked adverse pressure gradient and a relatively large suction near the trailing edge.

Even for such 'non-smooth' thickness distributions, thin-wing theory gives fair results. It has, however, been found that a form of second-order inviscid perturbation theory (not-so-thin wing theory) gives much

(Over)

A.R.C. C.P. No.774

533.6.048.2 :
533.6.013.13 :
533.693.3 :
533.6.011.5

THE PRESSURE DISTRIBUTION AT ZERO-LIFT ON SOME SLENDER DELTA WINGS AT SUPERSONIC SPEEDS. Firmin, M. C. P.
November 1963.

The pressure distribution has been measured on the rear of a slender delta wing with rhombic cross-sections as part of a programme to investigate the influence on the wave drag of thickness distributions that give rise to a marked adverse pressure gradient and a relatively large suction near the trailing edge.

Even for such 'non-smooth' thickness distributions, thin-wing theory gives fair results. It has, however, been found that a form of second-order inviscid perturbation theory (not-so-thin wing theory) gives much

(Over)

A.R.C. C.P. No.774

533.6.048.2 :
533.6.013.13 :
533.693.3 :
533.6.011.5

THE PRESSURE DISTRIBUTION AT ZERO-LIFT ON SOME SLENDER DELTA WINGS AT SUPERSONIC SPEEDS. Firmin, M. C. P.
November 1963.

The pressure distribution has been measured on the rear of a slender delta wing with rhombic cross-sections as part of a programme to investigate the influence on the wave drag of thickness distributions that give rise to a marked adverse pressure gradient and a relatively large suction near the trailing edge.

Even for such 'non-smooth' thickness distributions, thin-wing theory gives fair results. It has, however, been found that a form of second-order inviscid perturbation theory (not-so-thin wing theory) gives much

(Over)

more reliable results. Slender-wing theories, on the other hand, can be most misleading for such thickness distributions.

The second-order theory has also been applied to other thickness distributions and has been found to give more reliable results than thin-wing theory except near the wing leading edges where both methods fail.

more reliable results. Slender-wing theories, on the other hand, can be most misleading for such thickness distributions.

The second-order theory has also been applied to other thickness distributions and has been found to give more reliable results than thin-wing theory except near the wing leading edges where both methods fail.

Published by
HER MAJESTY'S STATIONERY OFFICE

To be purchased from
York House, Kingsway, London w.c.2
423 Oxford Street, London w.1
13A Castle Street, Edinburgh 2
109 St Mary Street, Cardiff
39 King Street, Manchester 2
50 Fairfax Street, Bristol 1
35 Smallbrook, Ringway, Birmingham 5
80 Chichester Street, Belfast 1
or through any bookseller

S.O. CODE No. 23-9015-74